RSC Advances

RSC Publishing

PAPER

View Article Online
View Journal | View Issue

Phosphatase-responsive amphiphilic calixarene assembly†

Cite this: *RSC Advances*, 2013, **3**, 8058

Yi-Xuan Wang, Dong-Sheng Guo, Yu Cao and Yu Liu*

Received 25th January 2013,
Accepted 19th March 2013

DOI: 10.1039/c3ra40453f

www.rsc.org/advances

A phosphatase-responsive supramolecular amphiphilic assembly was fabricated as an operationally targeted drug delivery carrier based on the host–guest complexation of amphiphilic calixarene with adenosine triphosphate (ATP). Remarkably, the complexation of calixarene with ATP lowers its critical aggregation concentration pronouncedly to form hollow spherical nanoparticles, which are identified by the combination of atomic force microscopy, high-resolution transmission electron microscopy and scanning electron microscopy. Moreover, the spherical assembly is efficiently responsive to phosphatase that is overexpressed in many tumor cells, and therefore the present system may have potential application in drug delivery systems.

Introduction

Stimuli-responsive assemblies have become an extraordinarily fascinating topic in recent years due to their foremost biological applications, especially as drug delivery vehicles.[1] The stimuli that make the assemblies practically operational include pH, temperature, light, magnetic fields, redox, ionic strength, as well as enzymes.[2] In this context, enzyme-responsive assemblies have emerged as an advantageous alternative for controlled release for the following reasons: (1) enzymes are involved in all biological processes and the enzyme-based approach exhibits excellent biocompatibility; (2) enzyme-catalyzed reactions are highly selective and efficient toward specific substrates for the targeted delivery of therapeutics to the enzyme-overexpression sites.[3] Up until now, many endeavors have concentrated on enzyme-triggered drug transport.[4] Zhang *et al.* have shown phosphatase-responsive supra-amphiphiles, utilizing the electrostatic interactions, to be potential carriers for cancer therapy.[5] We recently constructed a cholinesterase-responsive supramolecular vesicle as an operational targeted drug delivery system based on the concept of host–guest chemistry.[6]

Compared with conventional amphiphiles, supra-amphiphiles, which are constructed by noncovalent interactions or dynamic covalent bonds, are very simple to prepare and are tunably responsive to various external stimuli.[7] Besides the noncovalent interactions that often employed in building supra-amphiphiles, such as hydrogen-bonding, charge-transfer, and π–π interactions,[8] the host–guest strategy based on macrocyclic compounds is now attracting more and more interest. Cyclodextrin, sulfonatocalixarene, and cucurbituril macrocycles have been proven to be very biocompatible.[9] The host–guest complexation events based on such macrocycles occur commonly in aqueous media. Consequently, construction of supra-amphiphiles from these macrocycles is of fundamental interest for applications in biotechnology and medicine.[10]

In this work, we fabricated a phosphatase-responsive supramolecular amphiphilic assembly as an operationally targeted drug delivery carrier based on the host–guest complexation of amphiphilic calixarene (AC4AH) with ATP (Scheme 1). Calixarenes have been frequently used in building amphiphilic aggregations on account of their facile modification and intrinsic truncated-cone shape.[11] Moreover, the

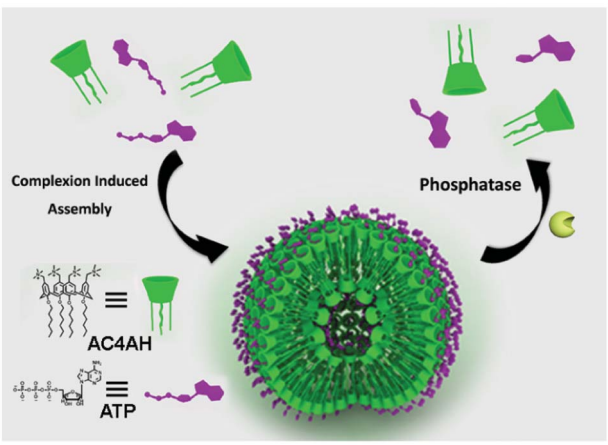

Scheme 1 Schematic illustration of the self-assembly of AC4AH with ATP and its phosphatase-response.

Department of Chemistry, State Key Laboratory of Elemento-Organic Chemistry, Nankai University, Tianjin 300071, P. R. China. E-mail: yuliu@nankai.edu.cn; Fax: (+86)22-2350-3625

† Electronic supplementary information (ESI) available: Experimental procedures and supporting figures. See DOI: 10.1039/c3ra40453f

desired rigidity of calixarene framework is beneficial to the stability of amphiphilic aggregation.[12] AC4AH, as an amphiphile with a host–guest recognition site,[13] spontaneously self-assembles into small micelles in aqueous media.[14] Remarkably, the complexation of AC4AH with ATP lowers its critical aggregation concentration (CAC) pronouncedly to form larger nanoparticles, and the complexed nanoparticle can be dissipated *via* the hydrolysis of ATP catalyzed by phosphatase. Phosphatase, which can catalyze the dephosphorylation of a variety of lipid phosphates, is overexpressed in many tumor cells such as ovarian cancer.[15] As a result, fabrication of phosphatase-responsive systems may lead to potential applications in targeted cancer therapy.

Experimental

Materials

ATP, adenosine diphosphate (ADP), adenosine monophosphate (AMP) and trimethylamine solution (30 wt% in water) were purchased from Aladdin and storage solutions of ATP and ADP were adjusted to pH 7.2 using NaOH aqueous solution (1 M). HPTS was purchased from Sigma-Aldrich. CIAP was purchased from Takara. All of these were used without further purification.

Synthesis of AC4AH

ClC4AH was synthesized and purified according to the procedures reported previously.[14,16]

AC4AH: A solution of 3.0 g (3.14 mmol) ClC4AH and 30 mL trimethylamine (30 wt% in water) in 70 mL of THF was stirred under argon at room temperature for 48 h. The solvent was removed *via* rotary evaporation under reduced pressure, and the resulting white precipitate was recrystallized twice from THF–H_2O yielding 2.2 g (59%) of AC4AH (Scheme 2). ^{1}H NMR (400 MHz, D_2O): δ = 6.97 (s, 8H), 4.27 (d, 4H), 4.16 (s, 8H), 3.80 (t, 8H), 3.41 (d, 4H), 2.75 (s, 36H), 1.88 (m, 8H), 1.28 (m, 24H), 0.81 (t, 12H). ^{13}C NMR (400 MHz, D_2O): δ = 13.89 (CH_3), 22.79 (CH_2), 25.92 (CH_2), 29.75 (CH_2), 30.25 (CH_2), 32.06 (CH_2), 51.96 (CH_3), 68.57 (CH_2), 75.48 (CH_2), 121.95 (C), 133.27 (CH), 135.35 (C), 157.91 (C). ESI-MS (*m*/*z*): Found: 559.3, 361.3, 262.5. Calculated: $[(M - 2Cl^-)/2]^+$ 559.4, $[(M - 3Cl^-)/3]^+$ 361.3, $[(M - 4Cl^-)/4]^+$ 262.2.

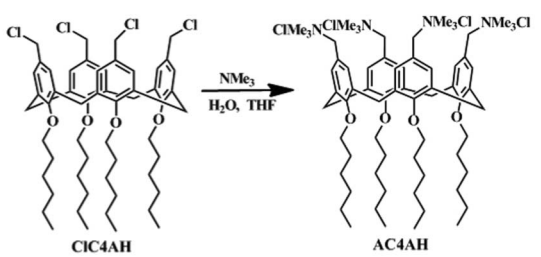

Scheme 2 Synthesis of AC4AH.

UV/Vis spectroscopy

The optical transmittance of the aqueous solution was measured in a quartz cell (light path 10 mm) on a Shimadzu UV-3600 spectrophotometer equipped with a PTC-348WI temperature controller.

Fluorescence spectroscopy

Steady-state fluorescence spectra were recorded in a conventional quartz cell (light path 10 mm) on a Varian Cary Eclipse equipped with a Varian Cary single-cell Peltier accessory to control the temperature (λ_{ex} = 339.0 nm, bandwidth(ex) = 2.5 nm, bandwidth(em) = 5.0 nm).

Isothermal titration calorimetry (ITC)

A thermostated and fully computer-operated isothermal calorimetry (VP-ITC) instrument, purchased from Microcal Inc., Northampton, MA, was used for all microcalorimetric experiments. All microcalorimetric titrations were performed in aqueous solution at atmospheric pressure and 298.15 K. Each solution was de-gassed and thermostated by a ThermoVac accessory before the titration experiment. Twenty-nine successive injections were made for the titration experiment. A constant volume (10 μL/injection) of AC4AH solution in a 0.250 mL syringe was injected into the reaction cell (1.4227 mL) charged with redistilled water.

TEM, high-resolution TEM, SEM, and AFM measurements

TEM images were recorded on a Philips Tecnai G2 20*S*-TWIN microscope operating at an accelerating voltage of 200 keV. High-resolution TEM images were acquired using a Tecnai 20 high-resolution transmission electron microscope operating at an accelerating voltage of 200 keV. The sample for TEM measurements was prepared by dropping the solution onto a copper grid. The grid was then air-dried. SEM images were recorded on a Hitachi S-3500N scanning electron microscope. The sample for SEM measurements was prepared by dropping the solution onto a coverslip, followed by evaporating the liquid in air. The samples for AFM were analysed using a multi-mode IIIa AFM (Veeco Metrology, USA) in tapping mode in air at room temperature. 2.0×10^{-5} M sample solutions were dropped onto newly clipped mica and then air-dried.

DLS measurements

The sample solution for DLS measurements was prepared by filtering the AC4AH solution through a 0.2 μm HT Tuffryn filter into a clean scintillation vial. The samples were examined on a laser light scattering spectrometer (BI-200SM) equipped with a digital correlator (TurboCorr) at 636 nm at a scattering angle of 90°. The hydrodynamic radius (Rh) was determined by dynamic light scattering experiments.

Results and discussion

AC4AH, appended concurrently with the hydrophilic quaternary ammoniums at the upper rim of calix[4]arene and the hydrophobic *n*-hexyl chains at its lower rim, displays the desired amphiphilic nature. Since the intrinsic cone shape of

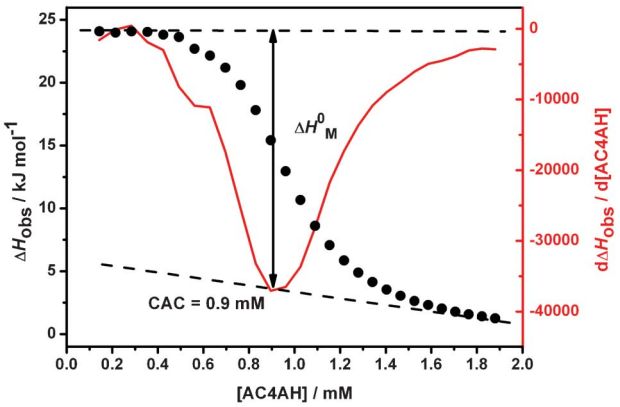

Fig. 1 Observed reaction enthalpy (ΔH_{obs}) *versus* the AC4AH concentration during microcalorimetric titration of 29 aliquots (10 μL) of a 10.27 mM solution of AC4AH into pure water at 298.15 K. The red line represents the first derivative of ΔH_{obs} against [AC4AH].

calixarene is the prerequisite for high-curvature aggregations of amphiphiles,[11] AC4AH is expected to form a micellar assembly. We performed an isothermal titration microcalorimetry (ITC) experiment to investigate the aggregation of AC4AH (Fig. 1). The micellization processes can be observed from enthalpograms, and the CAC value is determined as 0.9 mM from the first derivative of the enthalpy profile curve, which is in agreement with that evaluated by a well-established method based on pyrene fluorescence (Fig. S3, ESI†). According to the method by Garcia-Rio,[17] the aggregation number at the CAC was calculated as 13. Raston *et al.* have reported a similar calixarene with *n*-dodecyl alkyl chains at the lower rim. The formation of a small micelle (5.4 nm) was confirmed using dynamic laser scattering (DLS). Significantly, these kinds of calixarene derivatives are demonstrated to be biocompatible.[18]

ATP, a universal energy source that is phosphatase-active, plays an essential role in most biological processes.[19] We herein combined ATP and AC4AH to fabricate a supra-amphiphile that specially and efficiently targets phosphatase. AC4AH has a positive charge of four, while ATP has a negative charge of four, and therefore, the host–guest 1 : 1 molar ratio is considered to be suitable for assembly from the viewpoint of the charge compensation. The AC4AH–ATP molar ratio was maintained at 1 : 1 in all the following experiments. As a result of amphiphilic aggregation, the optical transmittance decreases gradually with increased concentration (Fig. 2a), and the CAC value was evaluated as 0.02 mM according to the plot of optical transmittance at 450 nm (Fig. 2b). Control experiments, replacing ATP by ADP and AMP, were performed (Fig. S4, ESI†), and the optical transmittance exhibited no appreciable decrease, indicating that the three sequential phosphate groups in ATP are crucial to induce the amphiphilic aggregation of AC4AH. Free AC4AH cannot generate obvious aggregation in the concentration region from 0.005 to 0.04 mM, which is also proved using DLS (Fig. 3a). It is therefore inferred that the complexation of AC4AH with ATP leads to the CAC decrease of the AC4AH amphiphile.

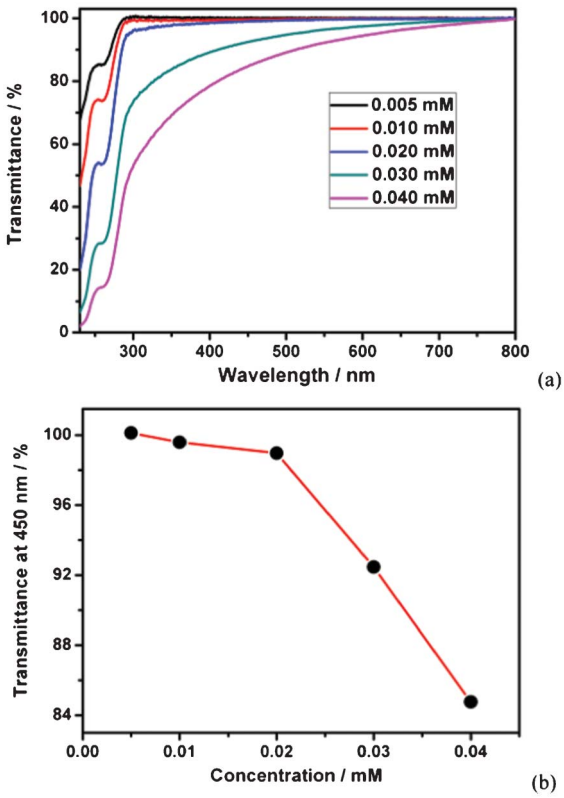

Fig. 2 (a) Optical transmittance of AC4AH–ATP complex by increasing the concentration from 0.005 mM to 0.04 mM at 25 °C in water. (b) Dependence of the optical transmittance at 450 nm on the complex concentration at 25 °C.

^{1}H NMR measurements were performed to determine the complex structure. As shown in Fig. 4a, the proton signals of adenine exhibited merely slight upfield shifts, which demonstrate that the adenine group should not penetrate into the calixarene cavity. Otherwise, the adenine protons would undergo prominent upfield shifts owing to the ring current effect of the aromatic nuclei of calixarene. The NMR result further validated the conclusion that the multivalent charge interactions between the phosphate groups in ATP and the quaternary ammonium groups in AC4AH play an absolutely dominant role in the host–guest complexation. Four phosphate groups are orientated on the upper rim of AC4AH comprised of four quaternary ammonium groups, which is unfavorable for adenine to enter into the calixarene cavity.[20] This is consistent with preliminary molecular mechanics calculations (Fig. 4b).

DLS, transmission electron microscopy (TEM), scanning electron microscopy (SEM) and atomic force microscopy (AFM) were employed to identify the assembly size and morphology of the AC4AH–ATP complex. In DLS measurements, particles formed by the complex exhibit a narrow size distribution with a hydrodynamic radius (R_h) of 247 nm at a scattering angle of 90° (Fig. 3b). The SEM image shows the spherical particles with a diameter ranging from 200–300 nm (Fig. 3c), in nice agreement with the DLS result. We can also see uniform spherical particles in the TEM image (Fig. 3d, S5, ESI†). The

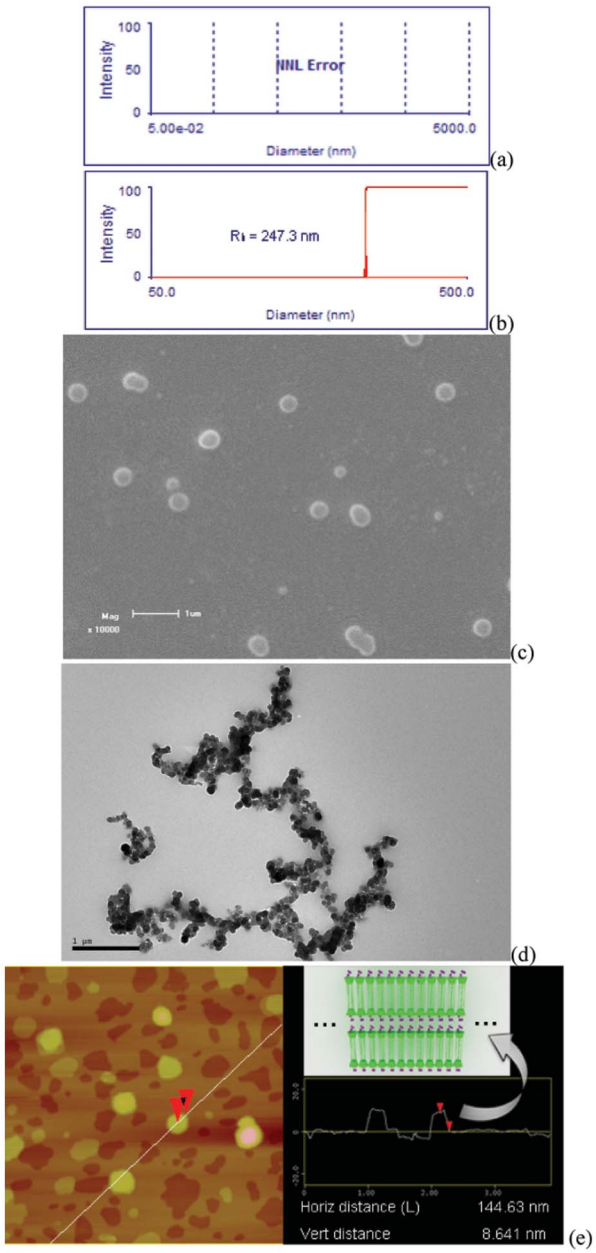

Fig. 3 (a) DLS data of AC4AH (0.02 mM). (b) Hydrodynamic diameter of the complex. (c) SEM image (the scale bar is 1 μm). (d) High-resolution TEM image (the scale bar is 1 μm). (e) AFM image and schematic illustration of two overlapping bilayer membrane.

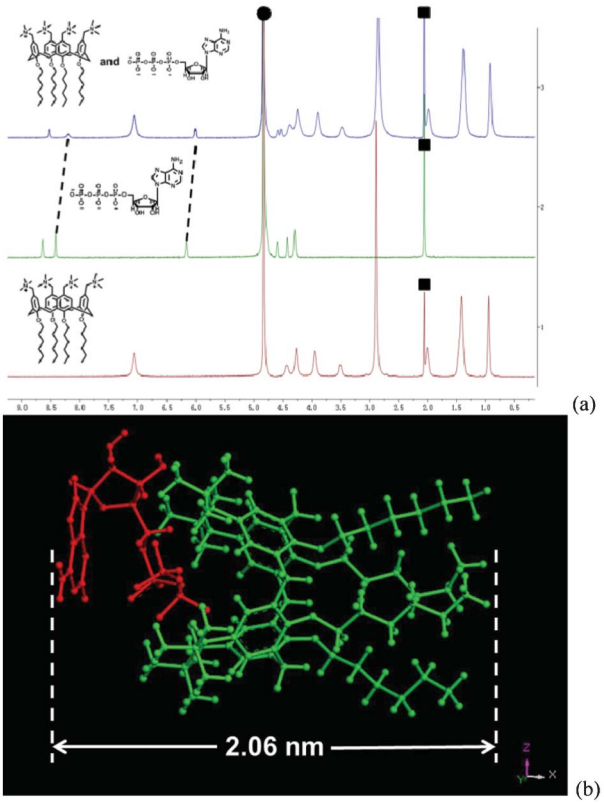

Fig. 4 (a) ^{1}H NMR spectra of AC4AH, ATP and the AC4AH–ATP complex in D_2O (5 mM). Acetonitrile was added as an external reference. The solvent (H_2O) and acetonitrile are denoted as symbols ● and ■, respectively. (b) Energy-minimized structure of the AC4AH–ATP complex obtained by a molecular modeling study. The geometry was optimized by the molecular mechanics method with a Dreiding force field.

AFM image (Fig. 3e) of the dried particles shows a height-to-diameter ratio of up to 1 : 30, indicating a thin-layered and collapsed hollow sphere structure.[21] Considering that the length of the AC4AH–ATP complex with fully extended alkyl tails is 2.06 nm obtained from molecular modeling (Fig. 4b), the height of the two overlapping membranes observed using AFM is almost equal to the height sum of the four complexes, which positively proves that the obtained hollow spheres possess a bilayer structure. Combining all the aforementioned results, we deduce that AC4AH–ATP complexes form supramolecular binary hollow spherical particles as schematically illustrated in Scheme 1.

For phosphatase-triggered disassembly, we keep the concentration of alkaline phosphatase (CIAP) at 0.15 U mL^{-1}, which is comparable with the average amount present in a healthy adult.[5] Upon addition of CIAP, the scattering intensity decreased rapidly (Fig. 5a). To exclude the possibility that CIAP itself is a factor leading to the disassembly of the particle, a control experiment was carried out in which the same amount of denatured CIAP (treated in boiling water for 3 h) was added to the AC4AH–ATP solution. Although the scattering intensity increases somewhat in the presence of denatured CIAP, no appreciable change as a function of time is observed. This clearly shows that enzymatic activation is achieved and required for particle disassembly. After the addition of CIAP for 30 min, the scattering intensity is much weaker and the diameter decreases observably (Fig. 5b), which reveals that most particles have been dispersed within 30 min. Furthermore we could not observe any sphere morphology in TEM image after CIAP treatment (Fig. 5b).

We further performed fluorescence measurements to monitor the complexation of AC4AH with ATP and the enzymatic reaction.[22] 8-Hydroxypyrene-1,3,6-trisulfonic acid

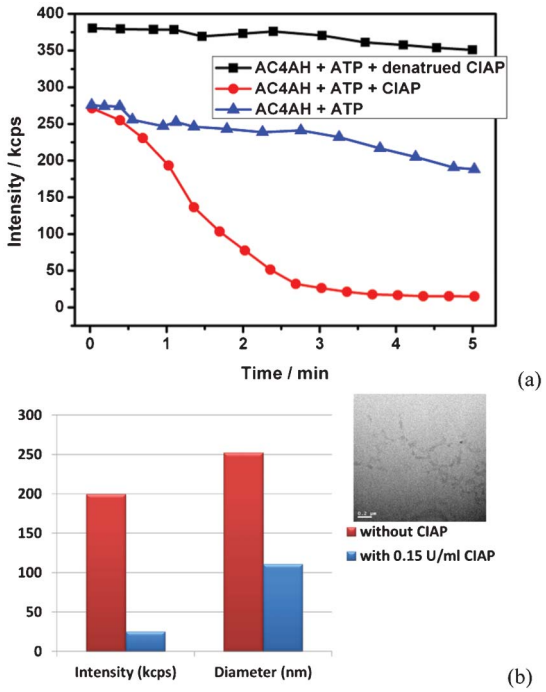

Fig. 5 (a) Dependence of the scattering intensity of AC4AH–ATP particles on time in the absence of CIAP, in the presence of CIAP and with denatured CIAP. (b) Magnified DLS datum of the AC4AH–ATP assembly in the absence and presence of CIAP for 30 min.[23] Inset: TEM image of the AC4AH–ATP particles after addition of CIAP for 30 min.

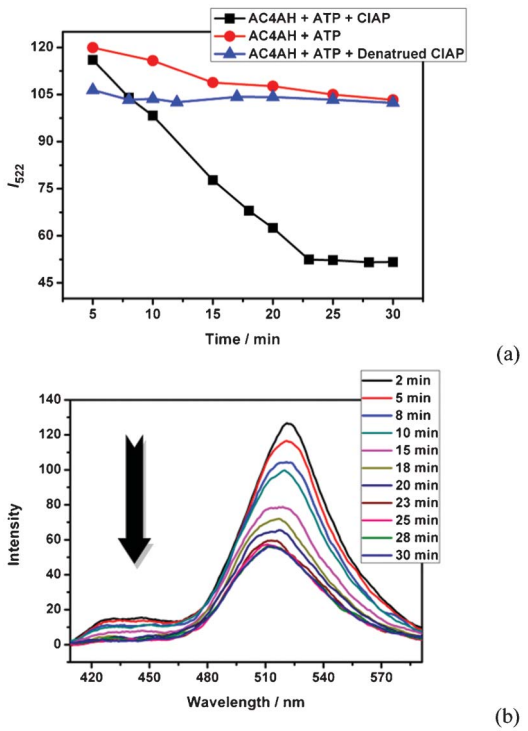

Fig. 6 (a) Dependence of the fluorescence intensity at 522 nm of HPTS (0.01 mM) with the AC4AH–ATP complex on reaction time in the absence of CIAP, in the presence of CIAP and with denatured CIAP; the excitation wavelength was 339 nm. (b) Fluorescence emission spectra of HPTS with AC4AH–ATP complex in the presence of CIAP.

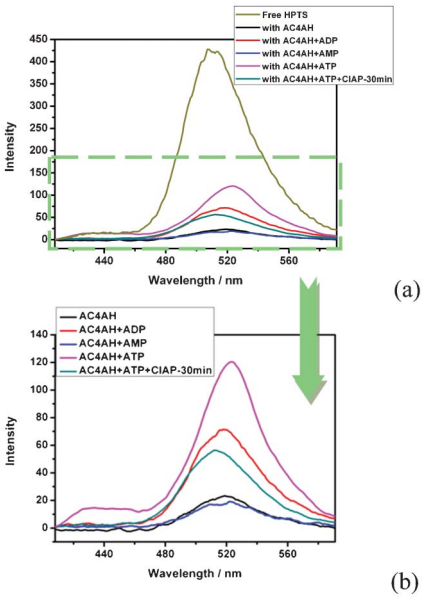

Fig. 7 (a) Fluorescence emission spectra of free HPTS, HPTS with AC4AH, AC4AH + ADP, AC4AH + AMP, AC4AH + ATP, and AC4AH + ATP after CIAP treatment. (b) Magnified figure without free HPTS.

(HPTS) was employed as the competitive dye with respect to its water solubility, multi-negative-charge, and satisfactory fluorescence. Upon addition of AC4AH, the fluorescence of HPTS was quenched 95% by the complexation of AC4AH (Fig. 7). It is well known that calixarenes are robust fluorescence quenchers.[24] Upon further addition of ATP, ADP, or AMP, the fluorescence of HPTS was quenched 75%, 84%, and 95%, respectively. The distinguishable fluorescence recoveries in the presence of nucleotides are a result of competitive binding. Accordingly, the enzymatic conversion of ATP (strong competitor) to ADP and AMP (weak competitors) can be easily monitored with the AC4AH–HPTS pair. As shown in Fig. 6, the fluorescence intensity of HPTS with the AC4AH–ATP complex decreased pronouncedly upon addition of CIAP. The ultimate fluorescence intensity after CIAP treatment is weaker than that with the AC4AH–ADP complex. This confirmed that ATP had been hydrolyzed to ADP and AMP in 30 min and the AC4AH–ATP assembly was then dispersed since ADP and AMP cannot induce AC4AH aggregation under such conditions.

Conclusions

In conclusion, we have fabricated a supramolecular binary hollow spherical assembly in virtue of the complexation of AC4AH with ATP. Two valuable factors of the AC4AH amphiphile have been definitely refined by ATP: its CAC decreases pronouncedly by over an order of magnitude; free AC4AH can merely form a small micellar assembly. Furthermore, the spherical assembly is efficiently responsive to CIAP that triggers the assembly to disperse *via* the hydrolysis of ATP. We believe that the reversible nature of

the noncovalent assembly and the special enzyme-response will promise substantial applications in drug delivery systems.

Acknowledgements

This work was supported by the 973 Program (2011CB932502), NSFC (20932004, 21172119), which are gratefully acknowledged.

Notes and references

1 (*a*) K. Wang, D.-S. Guo, X. Wang and Y. Liu, *ACS Nano*, 2011, **5**, 2880; (*b*) C. J. F. Rijcken, O. Soga, W. E. Hennink and C. F. van Nostrum, *J. Controlled Release*, 2007, **120**, 131; (*c*) Y.-F. Zhu, J.-L. Shi, W.-H. Shen, X.-P. Dong, J.-W. Feng, M.-L. Ruan and Y.-S. Li, *Angew. Chem., Int. Ed.*, 2005, **44**, 5083.

2 (*a*) D. Schmaljohann, *Adv. Drug Delivery Rev.*, 2006, **58**, 1655; (*b*) J. Du, Y. Tang, A. L. Lewis and S. P. Armes, *J. Am. Chem. Soc.*, 2005, **127**, 17982; (*c*) A. Almutairi, S. J. Guillaudeu, M. Y. Berezin, S. Achilefu and J. M. J. Fréchet, *J. Am. Chem. Soc.*, 2008, **130**, 444; (*d*) J. R. Kumpfer and S. J. Rowan, *J. Am. Chem. Soc.*, 2011, **133**, 12866; (*e*) L. M. Randolph, M.-P. Chien and N. C. Gianneschi, *Chem. Sci.*, 2012, **3**, 1363.

3 (*a*) J.-M. Hu, G.-Q. Zhang and S.-Y. Liu, *Chem. Soc. Rev.*, 2012, **41**, 5933; (*b*) Z.-M. Yang, G.-L. Liang and B. Xu, *Acc. Chem. Res.*, 2008, **41**, 315; (*c*) J. J. Shi, Z. Y. Xiao, N. Kamaly and O. C. Farokhzad, *Acc. Chem. Res.*, 2011, **44**, 1123; (*d*) N. Kamaly, Z. Xiao, P. M. Valencia, A. F. Radovic-Moreno and O. C. Farokhzad, *Chem. Soc. Rev.*, 2012, **41**, 2971.

4 (*a*) R. V. Ulijn, *J. Mater. Chem.*, 2006, **16**, 2217; (*b*) Z.-M. Yang, G.-L. Liang, L. Wang and B. Xu, *J. Am. Chem. Soc.*, 2006, **128**, 3038; (*c*) M. A. Azagarsamy, P. Sokkalingam and S. Thayumanavan, *J. Am. Chem. Soc.*, 2009, **131**, 14184; (*d*) N. Morimoto, N. Ogino, T. Narita, S. Kitamura and K. Akiyoshi, *J. Am. Chem. Soc.*, 2007, **129**, 458; (*e*) R. J. Amir, S. Zhong, D. J. Pochan and C. J. Hawker, *J. Am. Chem. Soc.*, 2009, **131**, 13949.

5 C. Wang, Q.-S. Chen, Z.-Q. Wang and X. Zhang, *Angew. Chem., Int. Ed.*, 2010, **49**, 8612.

6 D.-S. Guo, K. Wang, Y.-X. Wang and Y. Liu, *J. Am. Chem. Soc.*, 2012, **134**, 10244.

7 (*a*) X. Zhang and C. Wang, *Chem. Soc. Rev.*, 2011, **40**, 94; (*b*) Y. Wang, H. Xu and X. Zhang, *Adv. Mater.*, 2009, **21**, 2849.

8 (*a*) N. Kimizuka, T. Kawasaki, K. Hirata and T. Kunitake, *J. Am. Chem. Soc.*, 1998, **120**, 4094; (*b*) X. Zhang, Z. Chen and F. Würthner, *J. Am. Chem. Soc.*, 2007, **129**, 4886; (*c*) H. Ko, E. Kim, I. Hwang and K. Kim, *Chem. Commun.*, 2007, 1305.

9 (*a*) K. Wang, D.-S. Guo, H.-Q. Zhang, D. Li, X.-L. Zheng and Y. Liu, *J. Med. Chem.*, 2009, **52**, 6402; (*b*) V. D. Uzunova, C. Cullinane, K. Brix, W. M. Nau and A. I. Day, *Org. Biomol. Chem.*, 2010, **8**, 2037; (*c*) V. J. Stella and R. A. Rajewski, *Pharm. Res.*, 1997, **14**, 556.

10 (*a*) K. Kim, N. Selvapalam, Y. H. Ko, K. M. Park, D. Kim and J. Kim, *Chem. Soc. Rev.*, 2007, **36**, 267; (*b*) Y. Liu and Y. Chen, *Acc. Chem. Res.*, 2006, **39**, 681; (*c*) D.-S. Guo and Y. Liu, *Chem. Soc. Rev.*, 2012, **41**, 5907; (*d*) L.-X. Jiang, Y. Yan, M. Drechsler and J.-B. Huang, *Chem. Commun.*, 2012, **48**, 7347; (*e*) Y. Sun, Y. Yao, C.-G. Yan, Y. Han and M. Shen, *ACS Nano*, 2010, **4**, 2129; (*f*) Y. Sun, C.-G. Yan, Y. Yao, Y. Han and M. Shen, *Adv. Funct. Mater.*, 2008, **18**, 3981.

11 (*a*) M. Kellermann, W. Bauer, A. Hirsch, B. Schade, K. Ludwig and C. Böttcher, *Angew. Chem., Int. Ed.*, 2004, **43**, 2959; (*b*) Z. Wang, D.-S. Guo, J. Zhang and Y. Liu, *Acta Chim. Sin.*, 2012, **70**, 1709; (*c*) A. D. Martin, R. A. Boulos, K. A. Stubbs and C. L. Raston, *Chem. Commun.*, 2011, **47**, 7329; (*d*) A. D. Martin, E. Houlihan, N. Morellini, P. K. Eggers, E. James, K. A. Stubbs, A R. Harvey, M. Fitzgerald, C. L. Raston and S. A. Dunlop, *ChemPlusChem*, 2012, **77**, 308.

12 M. Lee, S.-J. Lee and L.-H. Jiang, *J. Am. Chem. Soc.*, 2004, **126**, 12724.

13 S. Shinkai, S. Mori, H. Koreishi, T. Tsubaki and O. Manabe, *J. Am. Chem. Soc.*, 1986, **108**, 2409.

14 (*a*) M. Strobel, K. Kita-Tokarczyk, A. Taubert, C. Vebert, P. A. Heiney, M. Chami and W. Meier, *Adv. Funct. Mater.*, 2006, **16**, 252; (*b*) N. Basílio, L. Garcia-Rio and M. Martín-Pastor, *Langmuir*, 2012, **28**, 2404.

15 (*a*) P. Meers, *Adv. Drug Delivery Rev.*, 2001, **53**, 265; (*b*) P. C. Kok, G. Venkatraman, D. Capatos and D. N. Brindley, *Chem. Rev.*, 2012, **112**, 5121.

16 V. G. Torgov, T. V. Us, T. M. Korda, G. A. Kostin, S. I. Miroshnichenko, O. V. Klimchuk and V. I. Kalchenko, *J. Inclusion Phenom. Macrocyclic Chem.*, 2008, **62**, 51.

17 N. Basílio and L. Garcia-Rio, *ChemPhysChem*, 2012, **13**, 2368.

18 P. K. Eggers, T. Becker, M. K. Melvin, R. A. Boulos, E. James, N. Morellini, A. R. Harvey, S. A. Dunlop, M. Fitzgerald, K. A. Stubbs and C. L. Raston, *RSC Adv.*, 2012, **2**, 6250.

19 T. Noguchi, T. Shiraki, A. Dawn, Y. Tsuchiya, L. T. N. Lien, T. Yamamoto and S. Shinkai, *Chem. Commun.*, 2012, **48**, 8090.

20 Y.-H. Shi and H.-J. Schneider, *J. Chem. Soc., Perkin Trans. 2*, 1999, 1797.

21 (*a*) W. Tao, Y. Liu, B.-B. Jiang, S.-R. Yu, W. Huang, Y.-F. Zhou and D.-Y. Yan, *J. Am. Chem. Soc.*, 2012, **134**, 762; (*b*) J. Zou, B. Guan, X.-J. Liao, M. Jiang and F.-G. Tao, *Macromolecules*, 2009, **42**, 7465.

22 We have recently introduced the supramolecular tandem assay principle as a convenient method to monitor activity of acetylcholinesterase and choline oxidase. See: D.-S. Guo, V. D. Uzunova, X. Su, Y. Liu and W. M. Nau, *Chem. Sci.*, 2011, **2**, 1722.

23 In order to investigate the diameter after CIAP treatment, we used the strongest laser source.

24 D.-S. Guo, K. Wang and Y. Liu, *J. Inclusion Phenom. Macrocyclic Chem.*, 2008, **62**, 1.